

## The Impact of Organic Additives on Phase Transformation and Particle Size of Bayer Process Desilication Product

Dilini Seneviratne<sup>1</sup>, Hong Peng<sup>2</sup> and James Vaughan<sup>3</sup>

1. PhD Candidate

2. Advance Queensland Research Fellow

3. Senior Lecturer

The University of Queensland – Rio Tinto Bauxite & Alumina Technology Centre, School of Chemical Engineering, University of Queensland, Brisbane, Australia

Corresponding author: d.seneviratne@uq.edu.au

### Abstract

Organic additives are used to tune the morphology and particle size of crystals in the zeolite manufacturing industry. However, their impact on phase transformation and size distribution of desilication product (DSP, belonging to the zeolite family) in Bayer desilication has not yet been extensively studied. In order to probe this impact, crystallisation of DSP in the presence of fifteen organic additives was studied in a batch reactor using synthetic solution. The results indicate that certain additives effect the phase transformation of zeolite A to sodalite and the particle size distribution of DSP produced. Solids samples were characterized using x-ray diffraction, scanning electron microscopy and their particle size distributions were measured using an AccuSizer particle counter.

**Keywords:** Organic additives, desilication product, crystallization, Bayer process.

### 1. Introduction

Reactive silica in bauxite, predominantly in the form of kaolinite and quartz, react in the Bayer process, driving silicate into solution. Once a critical supersaturation is reached, this silicate combines with other aqueous species to re-precipitate in the form of sodium aluminosilicates or zeolites known as desilication product (DSP). DSP precipitation, referred to as desilication, reduces silicate levels in process liquor, preventing silica contamination of gibbsite product, and is therefore an important step in the Bayer process. However, DSP can form unwanted scale, and also consumes valuable caustic and aluminium which exit the Bayer cycle as residue along with other minerals.

Bayer DSP types found in industry are predominantly in the form of sodalite and cancrinite [1]. However, these are known to form through a series of solution mediated phase transformations. These metastable transformations begin with an amorphous sodium aluminosilicate phase which converts to zeolite A, then to sodalite and then to cancrinite [2]. Desilication can occur in pre-desilication or digestion, depending on the configuration and reaction conditions of the Bayer plant. In synthetic solutions where silicate is introduced as aqueous  $\text{Na}_2\text{SiO}_3$ , at pre-desilication conditions (90 °C) as in this study, these transformations are slower and phase transformations can be clearly differentiated.

DSP precipitation control through the use of additives has been investigated to predominantly control scale formation. Commercial additives exist which have proven to reduce scaling by modifying liquor solubility properties [3, 4]. The Bayer process has also employed organic additives in the form of crystal growth modifiers (CGMs) to improve gibbsite precipitate properties for example to increase crystal size, reduce fines and to improve yield [5]. Modifying Bayer DSP crystal morphology through the use of CGMs has not yet been extensively investigated.

The research into modification and synthesis of various types of zeolites for industrial use, has a long history. This is due to their many varied and valuable chemical properties which are predominantly determined by their morphology. These properties are utilized in a number of industries including petrochemicals and detergents and include; ion-exchange ability, sorption capacity, shape selectivity and catalytic activity [6].

Through this research a number of additives have been shown to impact the crystallization of zeolites. Zeolites are typically synthesized in a strong basic medium which assists in the mineralization of silicate and aluminate species in reactant gels [7]. Organic structure-directing agents and seed assisted synthesis of zeolites are commonly employed to direct their formation, for example to stabilize the framework of zeolite molecular sieves [8]. Synthesis methods of various zeolite types have been historically patented, for example that of large zeolite crystals (up to 100  $\mu\text{m}$ ) through gel crystallization using an organic nitrogen compound additive [9]. In zeolite manufacturing, cations have been shown to influence anionic species present in solution and dissolved quaternary organic ammonium bases (such as tetraethyl ammonium bromide, TEAB) have been used as charge compensating cations in zeolite synthesis to modify morphology from as early as 1961 [10]. These organic compounds could have a significant impact on Bayer DSP and could be explored as pre-desilication additives to change DSP morphology.

Predicting the effect of modifying additives on crystal growth and morphology however, has proven to be difficult [11]. The range of organic additives chosen for this study was therefore kept broad to encompass common surfactants, polymers/flocculating agents, known Bayer impurities, organic acids, commercial reagents and zeolite CGMs. Myatt et al. tested a number of surfactants including sodium dodecyl sulfate (SDS), sodium dioctyl sulfosuccinate (DSS), cetyltrimethylammonium bromide (CTAB) and polyethylene glycol (PEG), observing the impact of these on zeolite A crystallisation [12]. These additives were found to increase the linear rate of crystal growth and sodium dioctyl sulfosuccinate was shown to reduce the number of nuclei produced. Sanhoob et al. investigated the effects of PEG on the pore structure of zeolite ZSM-12 and found that it played a significant role in controlling crystallization rate [13]. A medium size polyacrylic acid molecule (5200 MW) was also chosen, as this has shown to be effective in modifying oxalate crystal structure in previous studies under Bayer conditions [14].

## 2. Method

Initially, 12 additives were trialed as part of a scoping study and these are listed in Table 1. All were initially tested at 100 mg/L in batch stirred reactor tests. Cytec – Cyphos ionic liquid (IL) 101 was donated by Cytec and all other chemicals were purchased through Sigma Aldrich.

**Table 1. Organic additives tested in the scoping study.**

1	Citric acid
2	Cytec – Cyphos IL - 101 (IL - 101)
3	Guar
4	Humic acid
5	Malic acid
6	Polyacrylic acid (PAA) - 5200 MW
7	Polyethylene glycol (PEG) - 4000 MW and 8000 MW
8	Potato starch
9	Sodium acetate
10	Sodium dodecyl sulfate (SDS)
11	Sodium formate
12	Tetrabutylammonium chloride (TBAC)

Based on the findings from the initial scoping tests, where the anionic surfactant SDS showed the greatest impact on DSP crystal size distribution, secondary investigations on surfactants were conducted. Tests using the cationic surfactant CTAB, another anionic surfactant DSS and further tests at varying SDS concentrations were conducted. Additionally, TEAB, commonly used in zeolite manufacturing as a structure directing agent [15] was tested. The concentrations tested are summarized in Table 2. CTAB was purchased through Merck, and all other chemicals listed were purchased through Sigma Aldrich.

**Table 2. Organic additives tested in greater detail.**

Chemical	Nominal Target Concentrations (mg/L)
10 Sodium dodecyl sulfate (SDS)	25, 50, 250, 500, 750, 1000
13 Cetyltrimethylammonium bromide (CTAB)	50, 100, 500, 1000
14 Sodium dioctyl sulfosuccinate (DSS)	500
15 Tetraethyl ammonium bromide (TEAB)	250, 500

### 2.1. Batch Stirred Tank Reactor Tests

The batch reactor solution volume used was 300 mL, agitation was provided with an overhead stirrer at a rate of 300 rpm using an axial impeller with a diameter of 64 mm. Temperature was controlled to  $90 \pm 0.5$  °C by water bath heating. Reactors with an internal diameter of 105 mm, with baffle width 12 mm (four baffles) were used with a spacing of 32 mm between the bottom of the impeller and the reactor. Industrial Bayer process pre-desilication stage initial solution conditions were chosen with a composition of; 2M NaAl(OH)<sub>4</sub>, 5 M NaOH and 0.1 M Na<sub>2</sub>CO<sub>3</sub>.

Soluble sodium metasilicate was used to start each test at 0.1 M Na<sub>2</sub>SiO<sub>3</sub>. These target concentrations were produced by using 3 stock solutions; (1) 6 M NaAl(OH)<sub>4</sub>, 12 M NaOH, (2) 12 M NaOH, (3) Na<sub>2</sub>SiO<sub>3</sub> 100 g/L SiO<sub>2</sub> basis. Na<sub>2</sub>SiO<sub>3</sub> in solution will be expressed in terms of SiO<sub>2</sub> (g/L) in this study. For these scoping study experiments samples were taken at 1 and 4 hours following the addition of Na<sub>2</sub>SiO<sub>3</sub>. The further additive tests conducted shown in Table 2 used 300 and 500 mL batch reactor volumes and sampling was conducted between 15 minutes and 4 hours.

The solids samples collected were washed with de-ionised water to remove any associated additive before drying at 105 °C. The control (no additive) condition was repeated five times, and the solids and liquor were characterised, to determine repeatability of the batch reactor crystallization.

### 2.2. Shaker Bath Tests

The impact of the additives on solubility was determined using 100 mL 24 hour tests, where a shaker bath was used provide agitation and maintain constant temperature. PAA, SDS, TBAC, sodium acetate, sodium formate and humic acid were tested using this method. The same initial conditions as the batch reactor tests were used, also at 90 °C. The control condition where no additive was added was repeated four times, to determine experimental error of the 24 hour shaker test crystallisation.

### 2.3. Solids and Solution Characterisation

X-ray diffraction (XRD) patterns were recorded on a Bruker D8 Advance powder diffractometer using Cu K $\alpha$  radiation operating at a voltage of 40 kV and filament current of 40 mA.

Diffraction patterns were collected using  $\theta/2\theta$  geometry over a range of  $5 - 70^\circ$  at a scan rate of  $0.02^\circ 2\theta \text{ min}^{-1}$ . These results allowed investigation into the crystallinity of samples and the phases present. The peak intensity at  $2\theta = 7.2^\circ$  at any point divided by the final peak intensity at the same value, was used as an indication of crystallization of zeolite A by Myatt et al. [12]. However, for this study due to the meta-stable transformation of zeolite A to sodalite, sodalite formation must also be considered. To indicate the presence of hydroxy sodalite (SOD), the intensity at  $2\theta = 13.9^\circ$  was used (the raw area under this peak from  $13.7^\circ$  and  $14.1^\circ$  was calculated). To indicate the presence of zeolite A (ZA) the intensity at  $2\theta = 7.2^\circ$  was used (the raw area under this peak from  $7.0^\circ$  and  $7.4^\circ$  was calculated). The ratio between these areas was used as an indication of the extent of conversion of zeolite A to sodalite. Due to the influence of one of the additives tested, the formation of a third phase zeolite 21 (Z21) was also observed in sample XRD patterns. This type of zeolite structure was first defined and patented as zeolite N in 1968 [16] and is very similar to Z21 available in the 2015 XRD Powder Diffraction File spectrum database. A similar zeolite phase (zeolite LTN) was also observed by Buhl et al., in 2010 and was also referred to as NaZ-21 by Feng et al. in 2016 [17, 18].

Solutions were analysed for silicate concentration (expressed as g/L  $\text{SiO}_2$ ) using both inductively coupled plasma (ICP) mass spectrometry and the molybdate blue method [19] using an ultraviolet spectrophotometer (UV-Vis). Scanning electron microscopy (SEM) was carried out on solids samples using a JEOL-JSM-6460LA with a tungsten filament electron gun operated at a 10 kV beam current, a spot size of 50 and aperture of 1. Slurry samples collected from the batch reactor were diluted in Milli Q water and used for particle size distribution (PSD) analysis using an AccuSizer.

### 3. Results

#### 3.1. Initial Scoping Study

##### 3.1.1. Solubility and Yield

From the 4 and 24 hour solution silicate results, PAA, SDS sodium acetate and humic acid were shown to reduce the solubility of the DSP (within 95 % confidence intervals using the no additive case repeat test results). These results are summarised in Table 3. The addition of Na from the organic salts employed in these tests could also impact silicate solubility, however, this contribution ( $< 100 \text{ mg/L}$  of Na added) is the equivalent of  $< 0.004 \text{ M}$ , and negligible in this high ionic strength system.

A much higher variation in solution silicate concentration at 4 hours was seen for the repeated control conditions with no additive, due to kinetic effects having a greater impact at this stage. The yield results obtained showed a large variation in final solids mass ( $> 20 \%$ ) for the control tests. These preliminary solubility results therefore require confirmation, and a longer period of time to determine equilibrium solubility is recommended.

**Table 1. Solution  $\text{SiO}_2$  concentration as a function of time where initial  $\text{SiO}_2$  was 6 g/L.**

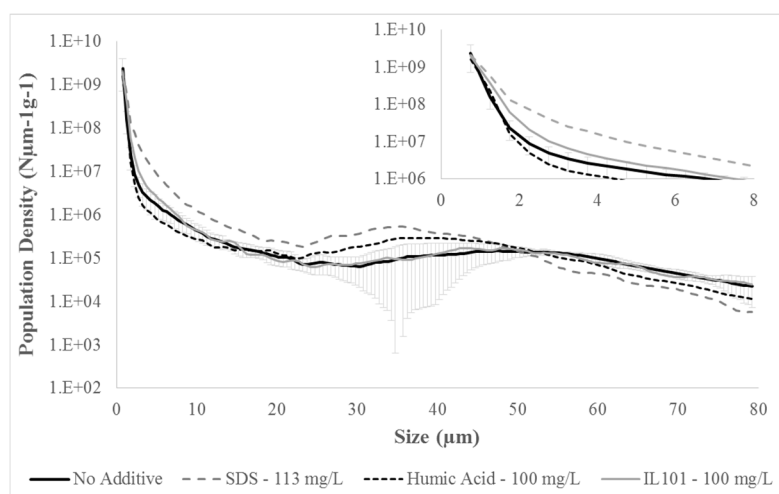
	$\text{SiO}_2$ (g/L)	
	4 hr ( $\pm 1.5$ )	24 hr ( $\pm 0.2$ )
None	4.3	1.9
PAA	2.8	1.1
SDS	3.3	1.3
Sodium Acetate	2.8	1.1
Humic Acid	2.6	1.3

### 3.1.2. XRD Results

The XRD results obtained for the control test conditions had an average ZA to SOD ratio of  $0.8 \pm 0.1$ . The 4 hour XRD results show that SDS (113 mg/L), humic acid (100 mg/L), malic acid (100 mg/L) and PEG 8000 MW (100 mg/L) enhanced the conversion of ZA to SOD (smaller ZA to SOD ratio) compared to the control repeat tests with a 95 % confidence interval. The maximum variation between the control experiments ZA to SOD ratio was 14 %.

### 3.1.3. Impact on Crystal Size Distribution and Morphology

A combination of SEM and AccuSizer data was used to determine the impact of these additives on the PSD produced. SEM analysis revealed that individual crystal sizes were below  $8 \mu\text{m}$  in all cases. Based on this finding, any particle greater than  $8 \mu\text{m}$  in size seen from AccuSizer data was interpreted as an agglomerate. The 4 hour samples from the control condition repeat tests were sized and the 95 % confidence interval variation in the batch reactor test PSD under the same conditions is shown in the error bars in Figure 1. The error range between 20 and  $50 \mu\text{m}$  appears larger due to the logarithmic y-axis. The proportional error introduced in terms of count of particles between 40 and  $80 \mu\text{m}$  is very high due to the small number of these particles present. The additives IL - 101, SDS and humic acid from the initial scoping study were identified as producing a different particle size distribution compared to the control. All other additives tested in this initial scoping phase were within the control test PSD range. Of these three additives, SDS and IL - 101 showed a significant reduction in fines ( $< 1 \mu\text{m}$ ), and an increase in the proportion of 1 -  $8 \mu\text{m}$  sized particles. SDS showed a significant increase in the proportion of  $> 8 \mu\text{m}$  particles, however, these were in the range of 8 to  $40 \mu\text{m}$  size agglomerates as shown in Figure 1.



Condition	Count D <sub>50</sub> (μm)	< 1 μm (Count %)	1 - 8 μm (Count %)	8 - 40 μm (Count %)	40 - 80 μm (Count %)	Volume D <sub>50</sub> (μm)
95% Confidence Interval	±0.2	±4.8	±4.5	±0.3	±0.2	±4.5
Control (No Additive)	1.1	89.8	9.4	0.5	0.4	59.5
SDS - 113 mg/L	1.4	68.5	30.2	1.0	0.3	47.4
Humic Acid - 100 mg/L	1.2	85.4	13.5	0.7	0.4	53.4
IL101 - 100 mg/L	1.2	78.8	20.4	0.4	0.3	59.2

**Figure 1. Particle size distributions obtained for control condition (no additive), SDS at 113 mg/L, humic acid at 100 mg/L and IL - 101 at 100 mg/L.**

An overall increase in the mean particle size (based on particle count) was observed from the SDS test, however, the mean size based on volume did not show an increase due to the decrease in particles  $> 40 \mu\text{m}$ , which have a much higher impact on overall sample volume.

The SEM images obtained were analyzed using the software package 'Image J', and the largest 10 crystals were sized for a range of images for each test case. The results of this analysis are given in Figure 2. The largest individual sodalite crystal size obtained for all of these tests were in the range of 1.9 to 3.7  $\mu\text{m}$  where IL - 101 and humic acid produced the largest sodalite crystals. This may indicate faster growth kinetics and may explain the reduced fines observed from the AccuSizer results, however, these are within the experimental error limits of the test. Similarly, 1.0 to 2.8  $\mu\text{m}$  zeolite A crystals were observed from these tests, where IL - 101 produced the largest zeolite A crystals.

No zeolite A was observed in the humic acid test case. For the SDS test however, a few larger zeolite type DSP were present and the largest size observed was 5.8  $\mu\text{m}$ . These zeolite phase crystals showed a hexagonal truncated face as shown circled in Figure 3 and were not visible in the other tests. Zeolite A generally has a cubic structure, whereas sodalite crystals have many curved platelets that appear to strap around each other, giving the appearance of balls of knitting wool as seen in Figure 3. As a result of this increased zeolite growth observed in the presence of SDS and the greatest reduction in fines, further testwork was conducted using SDS.

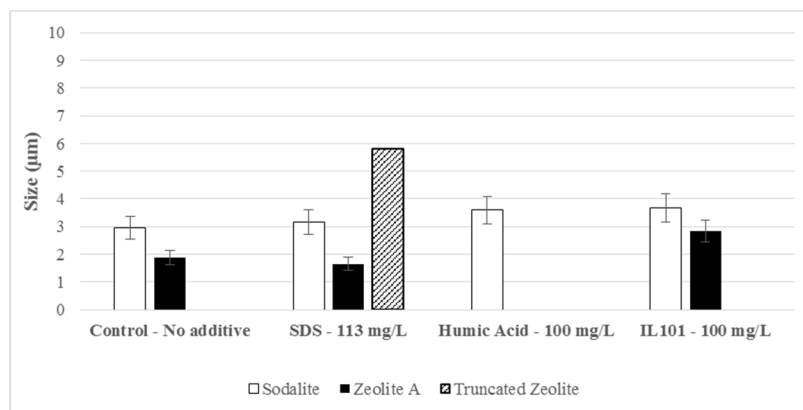


**Figure 2. SEM determined maximum individual crystal size.**

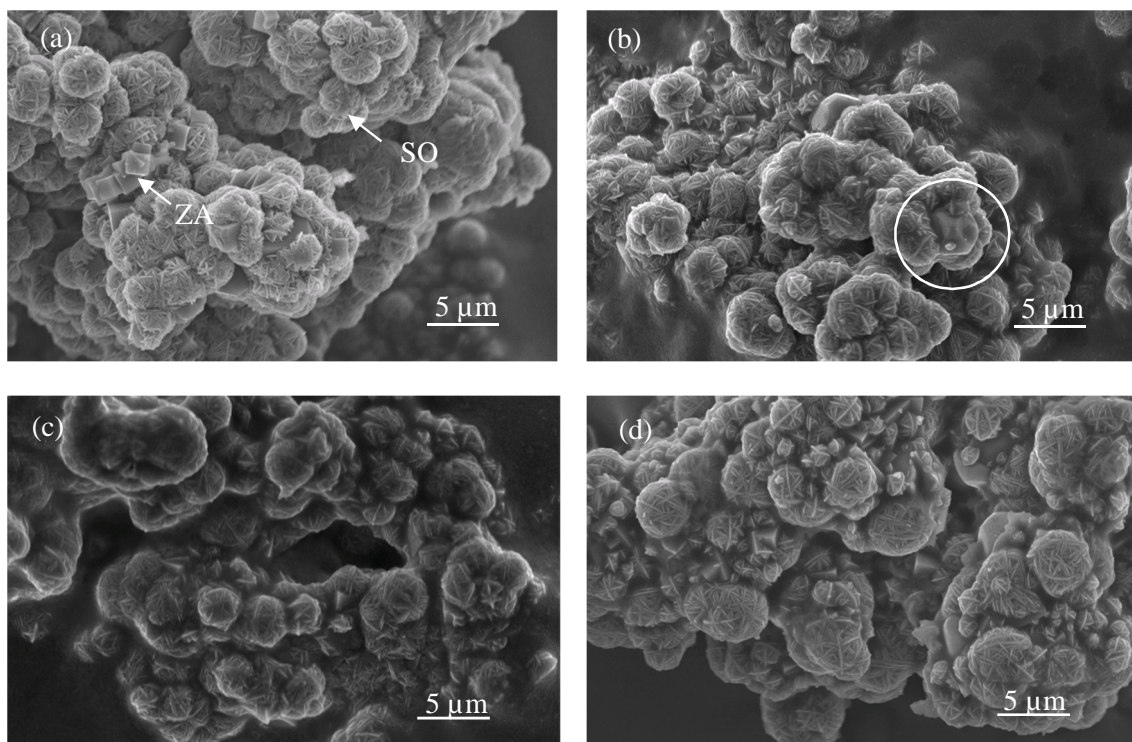


**Figure 3. SEM (a) control conditions no additive (b) SDS 113 mg/L (c) humic acid 100 mg/L (d) IL - 101 100 mg/L.**

### 3.2. Further Additive Testing

#### 3.2.1. Impact of SDS on Size Distribution and Morphology

Further tests were conducted at different SDS concentrations. Solution analysis showed no significant impact on final silicate concentration compared to the control with no additive within the 4 hour period for this series of tests. The particle size distributions obtained from these tests are shown in Figure 4. Steadily increasing SDS concentration did not increase its impact on the DSP PSD and the initial set of tests conducted at 25, 50, 113, 500 and 1000 mg/L showed that the 500 mg/L concentration had the greatest impact on changing the product PSD. A significantly higher proportion of particles between 1 and 40  $\mu\text{m}$  was observed at this concentration. However, the 1000 mg/L SDS condition showed similar results to the 25 mg/L test.

A repeat set of tests were conducted for the no additive condition and 250, 500 and 770 mg/L SDS concentrations. The no additive test PSD was within the previous no additive test range and all three SDS tests conducted showed a higher proportion of particles between 1 and 40  $\mu\text{m}$  very similar to the PSD obtained for the 500 mg/L test. However, the 700 mg/L test produced a PSD closest to the initial 500 mg/L test case. As shown in Figure 4, in all cases between 100 - 770 mg/L SDS, significantly less fines (< 1  $\mu\text{m}$ ) than the control condition with no additive and an increase in mean particle size by particle count was seen. SDS appeared to increase agglomeration between 8 - 40  $\mu\text{m}$  and enhanced crystal growth. However, due to the fewer 40 - 80  $\mu\text{m}$  particles produced in the presence of SDS, this change is not reflected in mean crystal size by volume.

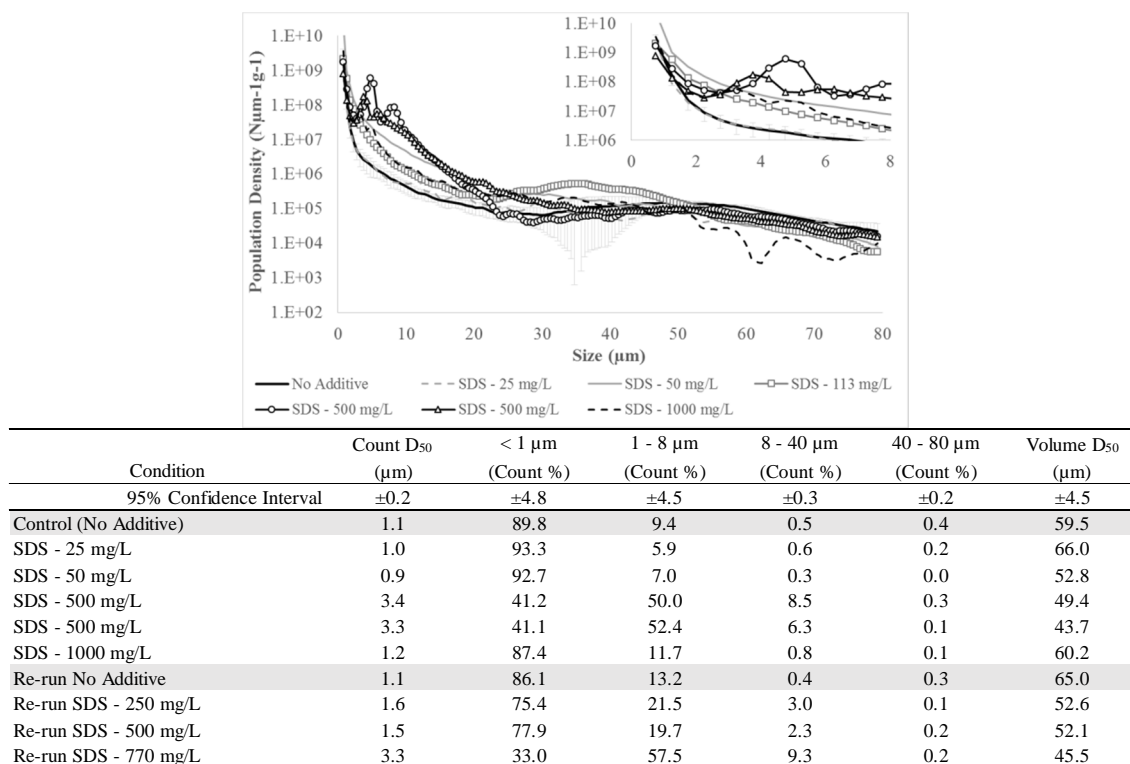


**Figure 4. Comparative particle size distributions for the control condition (no additive) and varying SDS concentrations.**

The initial 500 mg/L SDS test PSD showed slight peaks at around 5 µm and 8 µm which appeared to correspond to sodalite/zeolite A and the truncated zeolite phase respectively from SEM analysis (see Figure 5). The 500 mg/L repeat test showed peaks corresponding to 4 µm and 6.5 µm which again appeared to correspond to the sodalite/zeolite A crystals and the larger truncated zeolite phase respectively. Agglomeration effects indicated from the AccuSizer data should be investigated further and SEM analysis of the agglomerates formed is recommended.

The truncated zeolite phase was observed in all the preliminary SDS tests as shown in Figure 6. Time interval sampling revealed that large (~7 µm) zeolite crystals were seen as early as 15 minutes, and the hexagonal type structure was only seen to develop after 60 minutes. Additionally, the initial 500 mg/L SDS test showed a very narrow size distribution range for the sodalite, zeolite A and truncated zeolite phase, with an absence of fines from SEM analysis, which supports the AccuSizer findings. SEM analysis of the repeat tests conducted at 250, 500 and 750 mg/L SDS however, did not show any crystals with this truncated hexagonal structure and only zeolite A and sodalite were observed.

A total of eight tests were conducted at 500 mg/L SDS in this study to reproduce this zeolite with a hexagonal truncated face, however, this phase was not re-observed in significant quantities. All SEM results verified that the individual crystal size of the sodalite and zeolite A formed were coarser than the control condition (see Figure 7) between 250 and 770 mg/L SDS, indicating faster DSP crystal growth kinetics in the presence of SDS as supported by AccuSizer data.

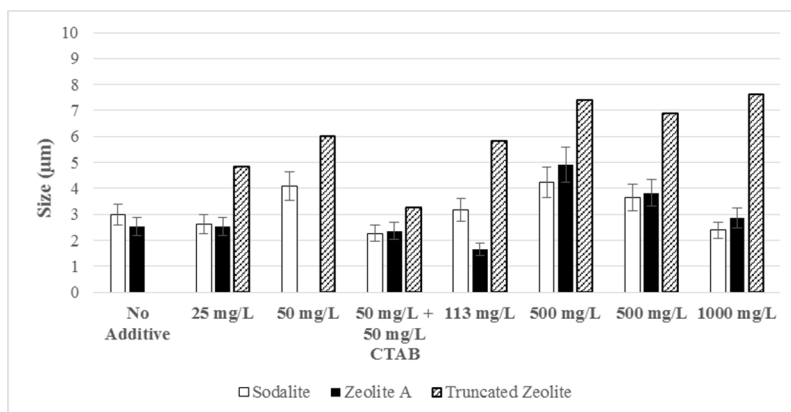


Figure 5. SEM image measured individual crystal size as a function of SDS concentrations.

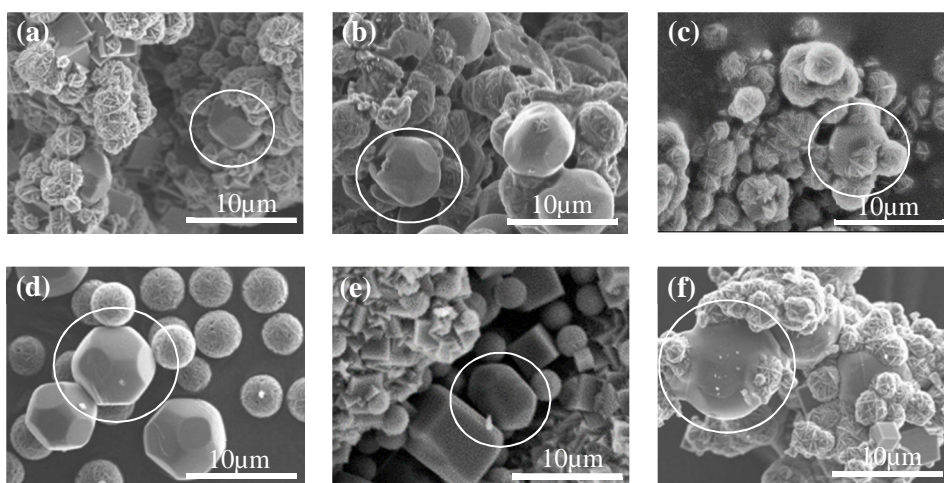


Figure 6. SEM results for varying SDS concentrations a) 25 mg/L SDS b) 50 mg/L SDS c) 113 mg/L SDS d) 500 mg/L SDS e) 500 mg/L SDS repeat f) 1000 mg/L SDS.

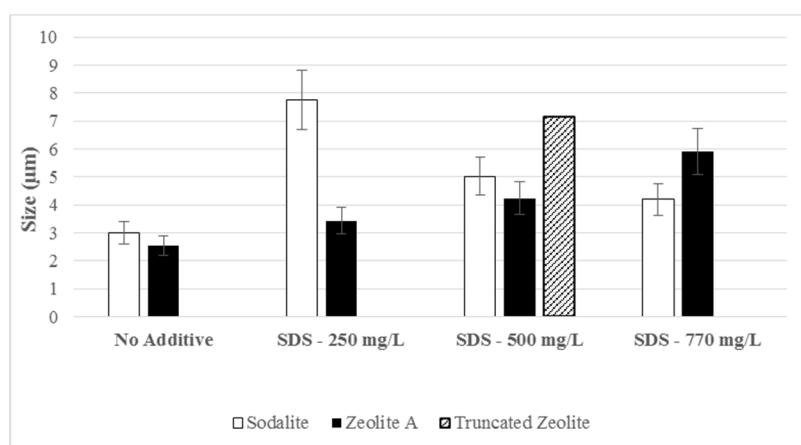
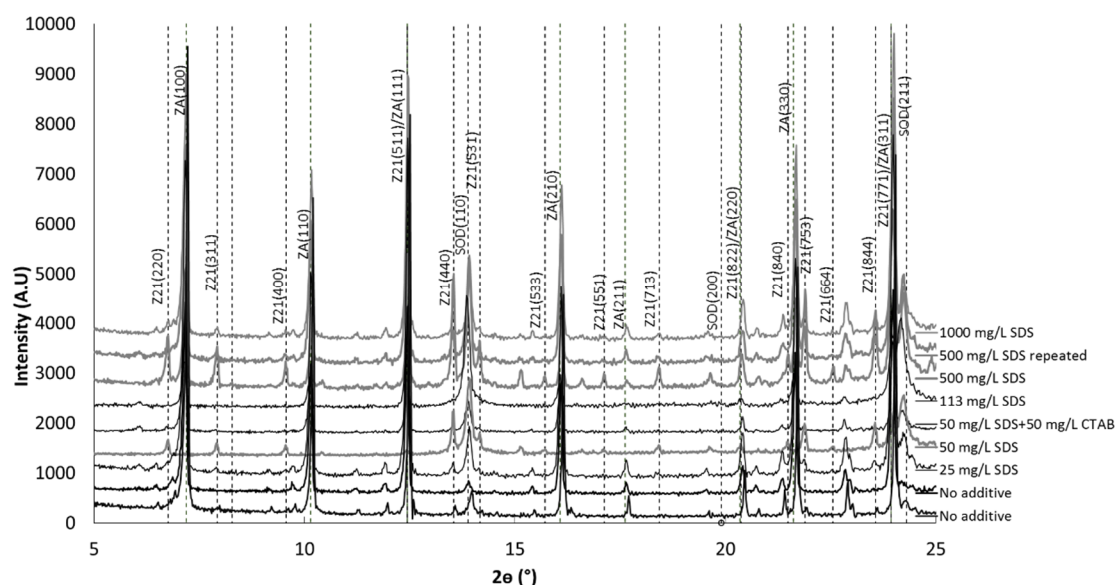


Figure 7. SEM image individual crystal size measured for SDS repeat testwork.

It should be noted that these batch reactor tests were not designed to optimize DSP growth, as the Si supersaturation was not maintained at a constant level. The impact on crystal growth could therefore be even more significant and could be explored further. For the cases of the 50

mg/L, initial and repeat 500 mg/L and the 1000 mg/L SDS tests, the truncated hexagonal zeolite face was abundant in the sample and resulted in a different bulk X-ray diffraction pattern.

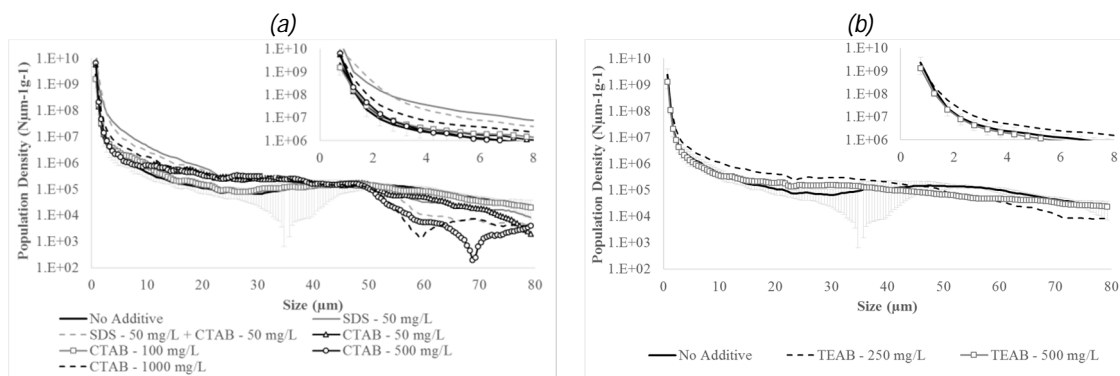
Figure 8 shows that these peaks correspond to peaks of Z21. Once in contact with caustic solution, SDS was observed to salt out at room temperature, as reported by Myatt et al. [12]. However, at 90 °C it was seen to partially re-dissolve. This can introduce greater variation in crystallisation conditions and may explain the inability to consistently reproduce the truncated zeolite phase obtained. Preliminary XRF and Leco analysis of the solids showed no indication that SDS was incorporated into the crystal lattice. It was also evident from the XRD data that SDS promotes the conversion of zeolite A to sodalite within the 4 hour test period.



**Figure 8. XRD spectrum results for varying SDS concentration tests, where ZA – zeolite A, Z21 – zeolite 21, SOD – hydroxy sodalite.**

### 3.2.2. Impact of CTAB, TEAB and DSS on Size Distribution and Morphology

The 4 hour particle size distributions obtained from CTAB tested at varying concentrations are compared to the no additive case in Figure 9. One test was conducted with a mixture of 50 mg/L SDS and 50 mg/L CTAB. The CTAB and SDS combined test, however, showed a reduced proportion of fines (< 1  $\mu\text{m}$ ), greater than that observed previously for the 50 mg/L SDS case. However, from SEM analysis larger individual crystal sizes were observed for the 50 mg/L SDS case as shown in Figure 5. From the series of CTAB tests, a significantly higher proportion of fines was observed for the 50 and 500 mg/L conditions and a corresponding decrease in the 1 - 8 and 40 - 80  $\mu\text{m}$  size ranges. This was not observed for the 100 mg/L case and no trend was observed. TEAB was tested at 2 concentrations and the 250 mg/L case showed a significant increase in 1 - 8 and 8 - 40  $\mu\text{m}$  size ranges with a corresponding reduction in fines.



Condition	Count D <sub>50</sub> (µm)	< 1 µm (Count %)	1 - 8 µm (Count %)	8 - 40 µm (Count %)	40 - 80 µm (Count %)	Volume D <sub>50</sub> (µm)
95% Confidence Interval	±0.2	±4.8	±4.5	±0.3	±0.2	±4.5
Control (No Additive)	1.1	89.8	9.4	0.5	0.4	59.5
SDS - 50 mg/L + CTAB - 50 mg/L	1.1	71.7	27.9	0.4	0.0	53.8
CTAB - 50 mg/L	0.9	95.8	3.7	0.4	0.1	55.7
CTAB - 100 mg/L	1.2	85.4	13.4	0.8	0.4	59.2
CTAB - 500 mg/L	0.9	95.1	4.4	0.4	0.1	57.8
CTAB - 1000 mg/L	1.0	88.6	10.8	0.5	0.1	57.6
TEAB - 250 mg/L	1.3	84.1	14.4	1.3	0.2	56.2
TEAB - 500 mg/L	1.2	88.4	10.4	0.9	0.3	63.5

**Figure 9. Particle size distributions for the control condition (no additive), CTAB (a) and TEAB (b) concentrations tested.**

The SEM determined coarsest individual particles sizes for the tests using CTAB, DSS and TEAB are shown in Figure 10. The SEM analysis showed no significant increase or decrease to the individual crystal size as a result of CTAB addition. DSS, another anionic additive was tested at 500 mg/L and showed no significant impact on Zeolite A crystal size, however, showed smaller sodalite crystal size. Of these, the TEAB additive showed a significant increase in the sodalite individual crystal size.

The SEM analysis also revealed a narrower size range of crystals compared to tests in this series. This was not reflected in the AccuSizer data for the 500 mg/L test case. XRD results from the CTAB tests indicate that CTAB may enhance the stability of zeolite A. From XRD, TEAB like SDS, appears to promote sodalite formation. Additionally, the sodalite structure from the TEAB tests look more interwoven and the sodalite platelets less regular. In general an aluminosilicate framework has a negative charge, however in this study, the charge of the additive appears to not be a consistent predictor of its impact on DSP.

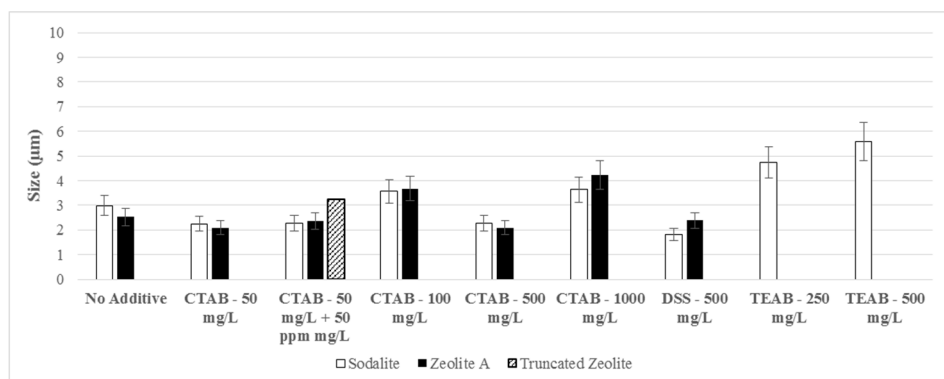


**Figure 10. SEM image measured individual crystal size for CTAB, DSS and TEAB tests.**

#### 4. Conclusions

Of the additives tested under Bayer predesilication conditions, both SEM and AccuSizer data have shown anionic surfactant SDS enhances individual DSP crystal growth when its concentration is between 250 to 750 mg/L. SDS within this concentration range was also shown to increase the proportion of agglomerates 8 - 40  $\mu\text{m}$  in size and reduce the proportion of DSP fines ( $< 1 \mu\text{m}$ ). In addition, a new intermediate phase with XRD peaks corresponding to zeolite 21 was formed when adding SDS, in contrast to the traditional DSP phase transformation pathway. However, the proportion of the zeolite 21 phase compared with zeolite A and sodalite phases was highly varied during the different concentrations and tests. The quaternary ammonium base TEAB also increased DSP crystal growth rate and reduced fines ( $< 1 \mu\text{m}$ ) at 250 mg/L. The ionic liquid IL - 101 was shown to reduce the proportion of DSP fines ( $< 1 \mu\text{m}$ ) at 100 mg/L. On the phase transformation DSP pathway, the results have shown humic acid, malic acid, PEG (8000 MW), SDS and TEAB enhance sodalite formation while CTAB conversely inhibits the conversion of zeolite A to sodalite.

#### 5. Acknowledgements

The authors would like to acknowledge Benjamin Foster and James Gudgeon, School of Chemical Engineering, University of Queensland as well as Matthew Iredale and Sharla Zhang, Department of Chemical Engineering, University of Bath for their contributions to this research. We gratefully acknowledge the financial support from the Queensland Government through the Advance Queensland Fellowship (Grant 15036). We also acknowledge the facilities and the scientific and technical assistance of the Australian Microscopy & Microanalysis Research Facility at the Centre for Microscopy and Microanalysis at The University of Queensland.

#### 6. References

1. J. Lowe, R. Hart, P. Smith, A. Rohl, and G. Parkinson, "Morphology and crystallinity: Insights into the mechanism of growth of DSP," in *Proceedings of the 7th International Alumina Quality Workshop*, p. 168, 2005.
2. T. Radomirovic, P. Smith, D. Southam, S. Tashi, and F. Jones, "Crystallization of sodalite particles under Bayer-type conditions," *Hydrometallurgy*, vol. 137, pp. 84-91, 2013.
3. D. Spitzer, O. Chamberlain, C. Franz, M. Lewellyn, and Q. Dai, "MAX HTTM sodalite scale inhibitor: plant experience and impact on the process," *Essential Readings in Light Metals: Alumina and Bauxite*, vol. 1, pp. 832-840, 2008.
4. M. Lewellyn, A. Rothenberg, C. Franz, F. Ballentine, F. Kula, L. Soliz, et al., "MAX HT" Bayer sodalite scale inhibitor: A green solution to energy," *Light Metals 2013*, p. 71, 2013.
5. J. Liu, D. Kouznetsov, J. Counter, and K. O'Brien, "Performance of new crystal growth modifiers in Bayer liquor," *Light Metals*, vol. 1, pp. 139-143, 2007.
6. L. B. McCusker and C. Baerlocher, "Zeolite structures," *Studies in Surface Science and Catalysis*, vol. 137, pp. 37-67, 2001.
7. C. S. Cundy and P. A. Cox, "The hydrothermal synthesis of zeolites: history and development from the earliest days to the present time," *Chemical Reviews*, vol. 103, pp. 663-702, 2003.
8. J. Grand, H. Awala, and S. Mintova, "Mechanism of zeolites crystal growth: new findings and open questions," *CrystEngComm*, vol. 18, pp. 650-664, 2016.
9. L. D. Rollmann and E. W. Valyocik, Mobil Oil Corporation, Manufacture of synthetic mordenite, *U.S. Patent 4,205,052*, 1980.
10. R. M. Barrer, *Hydrothermal chemistry of zeolites*: Academic Press, 1982.

11. F. Jones and M. I. Ogden, "Controlling crystal growth with modifiers," *CrystEngComm*, vol. 12, pp. 1016-1023, 2010.
12. G. J. Myatt, P. M. Budd, C. Price, F. Hollway, and S. W. Carr, "The influence of surfactants and water-soluble polymers on the crystallization of zeolite NaA," *Zeolites*, vol. 14, pp. 190-197, 1994.
13. M. A. Sanhoob, O. Muraza, E. M. Al-Mutairi, and N. Ullah, "Role of crystal growth modifiers in the synthesis of ZSM-12 zeolite," *Advanced Powder Technology*, vol. 26, pp. 188-192, 2015.
14. W. Fu, J. Vaughan, A. Gillespie, and N. M. Aroff, "Mechanisms of Polyacrylate Modified Sodium Oxalate Crystallization from Highly Alkaline Solutions," *Crystal Growth & Design*, vol. 16, pp. 1519-1530, 2016.
15. R. M. Barrer, "Zeolites and their synthesis," *Zeolites*, vol. 1, pp. 130-140, 1981.
16. N. A. Acara, Union Carbide Corporation, Zeolite n and process for preparing same. *U.S. Patent 3,414,602*, 1968.
17. J.-C. Buhl, L. Schomborg, and C. H. Ruescher, "Tetrahydroborate sodalite nanocrystals: Low temperature synthesis and thermally controlled intra-cage reactions for hydrogen release of nano- and micro crystals," *Microporous Mesoporous Materials*, vol. 132, pp. 210-218, 2010.
18. G. Feng, P. Cheng, W. Yan, M. Boronat, X. Li, J.-H. Su, et al., "Accelerated crystallization of zeolites via hydroxyl free radicals," *Science*, vol. 351, pp. 1188-1191, 2016.
19. D. F. Boltz and M. G. Mellon, "Determination of phosphorus, germanium, silicon, and arsenic," *Analytical Chemistry*, vol. 19, pp. 873-877, 1947/11/01 1947.

